ASAT
Military Technical College
CAIRO - EGYPT

A DISCRETE-VORTEX ANALYSIS OF UNSTEADY FLOW ABOUT CAMBERED PLATES

BY SAMIR I. M. MOSTAFA*
Egyptian Air Force

ABSTRACT

The evolution of a two-dimensional, incompressible, rapidly decelerating, viscous flow about a sharp-edged camber is simulated through the use of discrete-vortex method. An extensive study of the velocity field in the vicinity of the singular points led to the development of a novel method for the introduction of vorticity. The roll-up of the vortex sheets, the distribution of velocity and the pressure on the camber, and the drag force are calculated and compared with experiments.

INTRODUCTION

In the past decade many attempts have been made to use discrete vortex method (DVM) in many engineering problems. It has become clear that the solution of the Navier-Stoke's equation with the finite-difference or finite-elements method is not practical, especially for a high Reynolds number. Any grid-dependent method will face the same difficulties due to the fact that the boundary layer is proportional to $1/\sqrt{R_n}$, i.e a fine grid should be used as R_n increases, and a suitable turbulent model is required. In the discrete-vortex method turbulence is represented by a superposition of interacting vortices and no grid is required.

Flow induced structure vibration due to the shedding of vortices of bluff bodies, the effect of body vortices of the aerodynamics of missiles and aircrafts at high angles of attack, the effect of jumbo jet trailing vortices, and the study of the loading of bodies immersed in the pressure suppression pool of boiling water in a nuclear reactor are some of the problems investigated by the DVM. The present investigation is motivated by the phenomenon of the parachute collapse, a problem of great importance.

The previous models of parachute loads are based by and large on empirical assumptions(see Heinrich and Saari [1], and Mcwey [2]). The apparent mass is assumed to be a function of canopy projected

*Now Air Academy, Belbeis.

area only and is not a function of the prevailing flow characteristics. The vortex sheet analysis was used by Klimas [3] to derive the acceleration-independent apparent mass coefficient for arbitrarily shaped axisymmetric surfaces. Muramoto and Garard [4] used a continuous-source model to predict the steady-state drag of ribbon parachutes. None of the analyses dealt with the evolution of the unsteady wake and its interaction with the canopy.

The present work represents a fundamental study of the separated time-dependent flow about two-dimensional rigid cambered plates and offers a better understanding of the evolution of the wake under controlled conditions. The model presented herein removes the ambiguities with the use of the DVM and provides results which are in excellent agreement with those obtained experimentally.

MATHEMATICAL FORMULATION

The discrete-vortex method is basically a potential flow representation of incompressible high Reynolds number flow, which is essentially inviscid and irrotational except near the body boundary. Away from the body the flow is simulated by the interaction of vortices which were created near the separation points on the body. Near the boundary, the thin concentrated regions of vorticity emanating from the body at separation points are discretized into distinct vortices and convected with the main flow. The determination of the positions of creation and the strengths of the vortices is of fundamental importance to the model. Calculations of the convection velocities of vortices and the force acting on the body require a potential function representing the flow field.

One of the basic methods for studying the flow in a given region A is to transform that region by a conformal transformation to a "simpler" region B on which the problem can be solved or the flow is already known. The conformal transformation which transforms the cambered plate in the z plane to a circle in ζ plane is given as:

$$\zeta = \frac{z}{2} \pm \frac{1}{2}\sqrt{z^2 + 4b^2} - m \qquad (1)$$

and the inverse transformation is:

$$z = \zeta + m - \frac{b^2}{\zeta + m} \qquad (2)$$

It is easy to show that the camber in z plane is a circular arc of radius R = 1/m with its center at z_o such that

$$z_o = \frac{2m^2 - 1}{m}$$

where m is a geometrical parameter depends on the body shape, i.e. the camber angle α, fig.1.

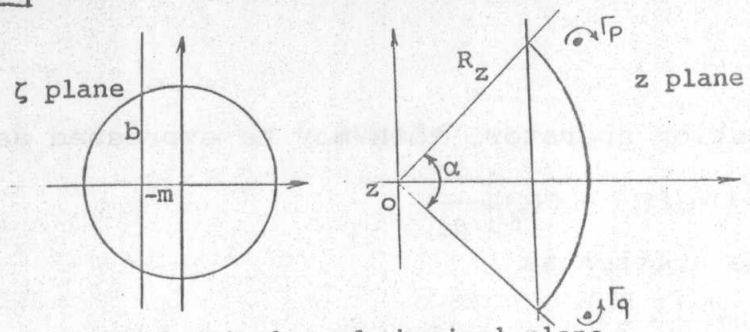

Fig.2. Circle and physical plane

The complex potential function in ζ plane of a circular cylinder placed in a stream whose velocity at ∞ is U(t), and 2m vortices shed from the cylinder is

$$W(\zeta) = -U(t)\left(\zeta + \frac{1}{\zeta}\right) + \frac{1}{2\pi}\sum_{k=1}^{2m}\Gamma_n\left[\mathrm{Ln}(\zeta-\zeta_\kappa) - \mathrm{Ln}\left(\zeta - \frac{1}{\bar{\zeta}_\kappa}\right)\right] \qquad (3)$$

in which $\Gamma_\kappa, \xi_\kappa$ represents respectively the strength and position of the k^{th} vortex . Equation (3) may be written in terms of z, as $\tilde{W}(z)$, if for each ξ the transformation function $\zeta = g(z)$, from equation (1), is used instead. The complex velocity of any point in the z plane is then calculated from $-u + iv = d\tilde{W}/dz$ or

$$\frac{d\tilde{W}}{dz} = \frac{dW}{d\zeta}\cdot\frac{d\zeta}{dz} \qquad (4)$$

where $d\zeta/dz$ is the transformation operator obtained from (2) as

$$\frac{d\zeta}{dz} = \frac{1}{2} \pm \frac{(z - z_o)}{2\sqrt{(z - z_o)^2 + 4b^2}} \qquad (5)$$

Complex Velocities:

Equation (3) may be written to represent m vortices, in ζ plane, , shed from each side of the camber, p the upper edge and q the lower edge, together with the most recent vortex at each side as:

$$\begin{aligned} W = &-U\left(\zeta + \frac{c^2}{\zeta}\right) + \frac{i\Gamma_{0p}}{2\pi}\mathrm{Ln}(\zeta - \zeta_{0p}) - \frac{i\Gamma_{0p}}{2\pi}\mathrm{Ln}\left(\zeta - \frac{c^2}{\bar{\zeta}_{0p}}\right) \\ &+ \frac{i\Gamma_{0q}}{2\pi}\mathrm{Ln}\left(\zeta - \frac{c^2}{\bar{\zeta}_{0q}}\right) - \sum_{k=1}^{m}\frac{i\Gamma_{kq}}{2\pi}\mathrm{Ln}(\zeta - \zeta_{kq}) + \sum_{k=1}^{m}\frac{i\Gamma_{kq}}{2\pi}\mathrm{Ln}\left(\zeta - \frac{c^2}{\bar{\zeta}_{kq}}\right) \\ &+ \sum_{k=1}^{m}\frac{i\Gamma_{kp}}{2\pi}\mathrm{Ln}(\zeta - \zeta_{kp}) - \sum_{k=1}^{m}\frac{i\Gamma_{kp}}{2\pi}\mathrm{Ln}\left(\zeta - \frac{c^2}{\bar{\zeta}_{kp}}\right) - \frac{i\Gamma_{0q}}{2\pi}\mathrm{Ln}(\zeta - \zeta_{0q}) \end{aligned} \qquad (6)$$

in which Γ_{op}, Γ_{oq}, ζ_{op}, ζ_{oq} are the strengths and locations of the most recent vortices (nascent vortices) shed at the two sides p and q of the camber and Γ_{kp}, Γ_{kq}, ζ_{kp}, ζ_{kp} are the strengths and positions of the k^{th} vortices at p and q edges.

Equation (4) gives the complex velocity at any non-vortical point in the z (physical) plane except at the points of singularity (at the two edges). To calculate the velocity at the center of a vortex one has to subtract the effect of that vortex from the complex potential function (as the vortex cannot induce velocity on itself) and carry out the differentiation for the remaining terms, [5]. For the k^{th} vortex whose center is at the position z_k, the complex velocity Pzk, $(-u + iv)$, may be obtained from

$$P_{zk} = \frac{d\tilde{W}(z)}{dz} - \frac{d}{dz}\left(\frac{i\Gamma_k}{2\pi}\cdot\mathrm{Ln}\ (z - z_k)\right)$$

Using the transformation operator, this may be expressed as

$$P_{zk} = \frac{dW}{d\zeta}\cdot\frac{d\zeta}{dz} - \frac{d}{d\zeta}\left[\frac{i\Gamma_k}{2\pi}\left(\mathrm{Ln}(f(\zeta) - f(\zeta_k))\right)\right]\frac{d\zeta}{dz}$$

The last term may be written as

$$\mathrm{Ln}(z - z_v) = \mathrm{Ln}(\zeta - \zeta_v) + \mathrm{Ln}\frac{f(\zeta) - f(\zeta_v)}{\zeta - \zeta_v}$$

substituting with $f(\zeta)$, $f(\zeta_k)$ from (2), and carrying out the differentiation, the velocity of the k^{th} vortex becomes

$$P_{zk} = P_{\zeta k}\cdot\frac{d\zeta}{dz} + \frac{i\Gamma_{kp}}{2\pi}\frac{(-b^2)(\zeta_{kp} + m)}{[(\zeta_{kp} + m)^2 + b^2]^2} \qquad (7)$$

Placement of the Nascent Vortex:

Equation (3) may be considered to represent the flow field at a certain instance of time t, where there are m vortices shed at each side of the camber. At time t+δt, when two new vortices (nascent) are introduced (shed), the flow field may be described by equation (6). From equation (4) the velocity, at the tip, may then be written as

$$\left.\frac{dW}{d\zeta}\right|_t = (-u_o + iv_o) + \frac{i\Gamma_{0p}}{2\pi}\left(\frac{1}{\zeta_t - \zeta_{0p}} - \frac{1}{\zeta_t - \frac{c^2}{\bar{\zeta}_{0p}}}\right) - \frac{i\Gamma_{0q}}{2\pi}\left(\frac{1}{\zeta_t - \zeta_{0q}} - \frac{1}{\zeta_t - \frac{c^2}{\bar{\zeta}_{0q}}}\right) \qquad (8)$$

This equation combines the effect of the two nascent vortices, namely Γ_{op}, Γ_{oq} with their images and with the effect of all other vortices and the ambient flow.

The fact that the flow separates tangentially with finite velocity at the edges of the plate (z_t) (Kutta condition) may be expressed by requiring that

$$\frac{dW}{d\zeta} = 0 \qquad \text{at } \zeta = \zeta_t = -m \pm ib$$

which indicates that the strengths and positions of the nascent vortices should induce, at the tip, a velocity equal in magnitude and opposite in direction to that induced by all other vortices, the doublet, and the uniform flow, i.e. $(-u_o + iv_o)$ in equation (8). Equation (8) represents two coupled equations for the strengths and positions of the nascent vortices and requires iterations. However, this iteration may be avoided if only one nascent vortex is considered (see Sarpkaya [5]).

Thus, for a p vortex one has

$$\frac{i\Gamma_0}{2\pi}\left(\frac{1}{\zeta_t - \zeta_0} - \frac{1}{\zeta_t - \frac{c^2}{\bar{\zeta}_0}}\right) + (-u_o + iv_o) = 0 \qquad (9)$$

Solving for the position ζ_o one gets

$$-\left(\frac{1}{\zeta_t - \zeta_0} - \frac{1}{\zeta_t - \frac{c^2}{\bar{\zeta}_0}}\right) = (-u_o + iv_o)\Big/\frac{i\Gamma_0}{2\pi} \qquad (10)$$

Separation Velocity:

According to Kutta condition the tangential velocity at the edge of the camber is finite. Using the complex version of the l'Hopital's rule [6] the finite velocity at the tips may be calculated from

$$\left.\frac{dW}{dz}\right|_{z=z_t} = \lim_{z \to z_t} (dw/d\xi)/(dz/d\xi) \qquad (11)$$

This gives

$$V_{tip} = \pm \frac{d^2W}{d\zeta^2} \cdot \left(\frac{ib}{2}\right) \qquad (12)$$

Time-Dependent Forces:

The force acting on the body may be calculated either through the integration of the pressure distribution around the body or through calculating the rate of change of impulse. Bernoulli's equation for unsteady flow is given by

$$\left(\frac{P_1}{\rho} + \frac{V_1^2}{2}\right) - \left(\frac{P_2}{\rho} + \frac{V_2^2}{2}\right) - \int_1^2 \frac{\partial V}{\partial t} ds = f(t)$$

where the indices indicate two points on the body, and f(t) accounts for the time rate of change of circulation since there is no pressure drop across the shear layer. The normalized differential pressure between two points m and n becomes

$$\frac{P_m - P_n}{\rho U_o^2/2} = \frac{V_{t1}^2 - V_{t2}^2}{U_o^2} + \frac{V_n^2 - V_m^2}{U_o^2} + \frac{\partial}{\partial t} \int_m^n 2 \frac{V}{U_o^2} ds \qquad (13)$$

The integration of the differential pressure between the upstream and downstream faces of the camber yields the force components.

METHOD OF CALCULATION

As shown in equations (9) and (11), the position ξ_o and the strength Γ_o of the nascent vortex should be related (through Kutta condition), to the rate at which the circulation is shed into the wake. Fage and Johansen [7] have indicated that the rate at which the vorticity is shed may be calculated as

$$\delta\Gamma/\delta t = 0.5\ (V_1+V_2)(V_1-V_2)$$

where V_1, V_2 are the velocity at the inner and outer edges of the shear layer. In the present investigation V_1 is calculated from equation (12) and V_2 is taken as the average velocity of three locations along the radial line passing through the tip, at r=1.05, 1.1, and 1.15.

The foregoing analysis indicates that the strength, the position, and the time increment are all crucial parameter in the DVM and have to be determined judiciously. The method used in the past

can be generally classified into two main categories. The first (see Clements [8,9], and Kuwahara [10]) used a fixed nascent vortex position near the separation point and calculate the velocity U_s at that point. The rate at which vorticity is shed from the point of separation is calculated from $\delta\Gamma/\delta t = 0.5\, U_s^2$, and the time interval δt is chosen arbitrarily with a fixed value throughout the calculations, (see also Kiya and Arie [11]).

Sarpkaya [5] was the first to use the second method which involves the use of variable nascent vortex position. He defined the velocity of the shear layer U_{sh} as the average of the transport velocity of the first four vortices, next to the edge, in the shear layer in order to calculate the rate of shedding of vorticity from $\delta\Gamma/\delta t = 0.5\, U_{sh}^2$. The positions of the nascent vortices are chosen to satisfy the Kutta condition at the edges of the plate. Thus, this method allows for interaction between the conditions in the wake and the point of appearance of the vortex.

None of the previous methods examined the effect of the point of placement of the nascent vortex on the velocity distribution in the neighborhood of the separation points, or calculated the vorticity flux based on the finite separation velocity at the sharp edges of the body. It is clear that ζ_o, Γ_o and δt cannot be chosen arbitrarily; the position of the nascent vortex directly affects the separation velocity V_1 and the sheet mean velocity $(V1+V_2)/2$, which in turn dictates the rate at which vorticity is shed into the wake.

To determine the most preferable nascent vortex position, and to establish a general method whereby the nascent vortices may be introduced into the flow field without any ambiguity for any sharp edged body, an original study was coducted. The tip region, in the physical plane, was discretized with a suitable grid and at each grid point ζ value of Γ_o nescessary to satisfy Kutta condition at the tip was determined and used to calculate the separation velocity V_1, the time interval, and the velocity profile along the radial line passing through the tip. Calculations have shown that there is, in fact, a finite region in which the nascent vortices may be introduced in order to produce a realistic velocity profile with its maximum nearly at the tip, and there is a unique position for each vortex strength that this maximum velocity becomes exactly at the tip, i.e. equals to the separation velocity V_1. It was concluded that for the case of a 120° camber the nascent vortices should be introduced at a radial distance of $r=1.0925$ and $\Theta=120 \pm 2.08°$ in the circle plane. For more details about the method see Mostafa [12].

The following outlines the steps used in the calculation:

1. Calculate the strength of the nascent vortices Γ_o from Kutta condition, Equation (10), in which the position of the vortex is a known fixed value;
2. Calculate the separation velocity V_1 at the two edges;

3. Calculate the velocity V_2 at the inner edge of the shear layer;
4. Calculate the time interval $\delta t = 2\Gamma_o/(V_1^2 - V_2^2)$;
5. Convect the two nascent vortices with the average velocity of the shear layer $V = (V_1 + V_2)/2$, and all other vortices with a second order convection scheme, for the time interval δt;
6. Calculate the flow characteristics and force coefficients;
7. Check the flow condition by examining values of V_1 and V_2:
   - if $V_1 - V_2 > 0.2$ repeat the foregoing steps
   - if $V_1 > V_2$ switch the angular positions of the fixed birth point to their image points, and calculate V_2 as the average velocity of the three radial locations at r = .95, .9, and .85, at the upstream side of the camber.

The forgoing steps are quite general and can be used for any camber in decelerating flow, having any velocity history, provided that the optimum points for placement of the nascent vortices are determined as described before.

NUMERICAL RESULTS AND PHYSICAL EXPERIMENTS

Calculations were carried out for time-dependent normalized velocity given as:

$U/U_o = 1$ for $T^* = U_o\, t/c \leq 8.65$,

and for $8.65 > T^* \geq 21.5$,

$$= 1 - 0.1539(T^* - 8.65) + 0.00531(T^* - 8.65)^2$$

which corresponds to that encountered in a series of experiments. Test were carried out on a thin cambered plate with a 1.5 inch radius and a 120° camber angle supported inside a vertical water tunnel with a 2ft X 2ft cross section and 17ft high. The fluid was initiated and controlled by a quick-release valve located at the bottom of the tank. The description of experimental equipment and testing procedures is very similar to that mentioned in [13] and will not be repeated here due to space limitations.

The computer program provided at specified times the positions of all vortices, the rate of shedding of vorticity from the edges of the camber, the velocity distribution on the upstream and downstream faces of the camber, the total and differential, pressure and the force coefficient. Fig.2 shows the evolution of the wake and the velocity field during the steady part of the flow, i.e. $T^* < 8.65$. As the flow separates from the two edges, the shear layer emanating from each separation point starts to roll on itself as the vorticity grows in the wake. With a sufficient number of vortices the two vortex clusters stretch themselves away from the camber creating more uniform distribution of velocity and pressure on the back side of the camber, Fig.3. During this period the locations of maximum velocity and minimum pressure move towards the central part of

the plate, and the velocity V2 and V1 change rapidly from an initial large value at the start of the motion to nearly constant. Following the onset of deceleration (for $T^*>8.65$) the current induced by the wake becomes more effective than the incoming flow and the velocity V2 at the inner edges of the shear layers increases while the separation velocity V1 decreases. In fact at $T^*\simeq12$ the velocities switch itself or the velocity induced by the returning wake becomes stronger than that induced by the nascent vortex and the incoming ambient flow, Fig.4. The differential pressure near the central part of the camber becomes increasingly negative, i. e. positive pressure is created on the downstream face of the camber, Fig.5. This enhanced by the backward motion of the wake, as the two large vortices drive themselves by their mutual induction creating a large velocity on the backside of the camber and increasing the region of the negative differential pressure. The locations of maximum velocity and minimum pressure move outward to the edges, creating large opposite sign vorticity as the induced flow separates on the backsides of the tips. A comparison is made between the calculated and photographed flow fields at corresponding times. Figures 6 and 7 show that the flow in the immediate vicinity of the camber (plotted to the same scale), exhibits excellent agreement between the calculated and experimental observations.

Fig.8 shows a comparison of the calculated (through pressure integration) and measured drag coefficients. In general the agreement between the calculated and the measured values is quite good. In time intervals between 13 and 16 and between 19 and 22 the calculated cd is somewhat larger. The reason is mainly due to the viscous effect as the vorticity dissipates in the wake. The drag coefficient as it continues to drop goes through zero value near the middle of deceleration, and attains its largest negative value near the end. Subsequently the force gradually approaches zero as the two large vortices wash away from the plate and the secondary velocity induced at the tip gradually decreases, Fig.9.

CONCLUSIONS

The present investigation dealt with a rapidly decelerating flow about a two-dimensional camber. A novel method for the introduction of vorticity, based on the finite velocity at the sharp edges, at variable time intervals was introduced and found to produce results in excellent agreement with those observed experimentally. The development of a negative differential pressure near the central part of the camber is thought to be primarily responsible for the inseption of the partial collapse of the parachutes at high rates of deceleration. It is hoped that the investigation presented herein will provide inspiration for the development of a more general vortex model with which the dynamics of axisymmetric, porous, and flexible parachute canopies can be investigated.

REFERENCES

1. Heinrich, H. G. and Saari, D. P., "Parachute Opening Shock Calculations with Experimentally Established Input Functions," J. Aircraft, Vol. 15, No. 2, pp. 100-105, (1978).
2. McWey, D. F. and Walf, D. F., "Analysis of deployment and Inflation of Large Ribbon Parachutes," J. Aircraft, Vol. 11, pp. 96-103, (1972).
3. Klimas, P. C., "Fluid Mass Associated with an Axisymmetric Parachute Canopy," J. Aircraft, Vol. 14, No. 6, pp. 577-580, (1977).
4. Muramoto, K. K., and Garrard, W. L., " A Method for Calculating the Pressure Field about a Ribbon Parachute Canopy in Steady Descent," AIAA 8th Aerodynamic Decelerator and Ballon Technology Conference, Hyannis, Mass., AIAA-84-0794, (1984).
5. Sarpkaya, T., "An Inviscid Model of Two-Dimensional Vortex Shedding for Transient and Asymptotically Steady Separated Flow over an Inclined Plate," J. Fluid Mech., Vol. 68, pp. 109-128, (1975).
6. Marsden, J. E., "Basic Complex Analysis," W.H. Freeman and Company, San Fransisco, (1973).
7. Fage, A., and Johansen, R. C., "The Structure of Vortex Sheets," Aero. Res. Council, R&M, No. 1143, (1928).
8. Clements, R. R.An Inviscid Model of Two-Dimensional Vortex Shedding," J. Fluid Mech., Vol. 57, pp. 321-335, (1973).
9. Clements, R. R., and Maull, D. J., " The Representation of Sheet of Vorticity by Discrete Vortices," Prog. Aerospace Sci., Vol. 16, No. 2, pp. 129-146, (1975).
10. Kuwahara, K., "Numerical Study of Flow Past an Inclind Flat Plate by an Inviscid Model," J. Phsical Soc. Japan, Vol. 35, pp. 1545-1551, (1973).
11. Kiya, M., and Arie, M., "A Contribution to an Inviscid Vortex -Shedding Model for an Inclined Flat Plate in Uniform Flow," J. Fluid Mech., Vol. 82, pp. 223-240, (1977).
12. Mostafa, I. M., "Numerical Simulation of Unsteady Separated Flows," Ph. D. Thesis, Naval Postgraduate School, Monterey, CA., (1987).
13. Sarpkaya, T., and Ihrig, C. J., "Impulsively Started flow about Rectangular Prisms: Experiments and Discrete Vortex Analysis," J. Fluid Engineering, Vol. 108, pp. 47-54, (1986).

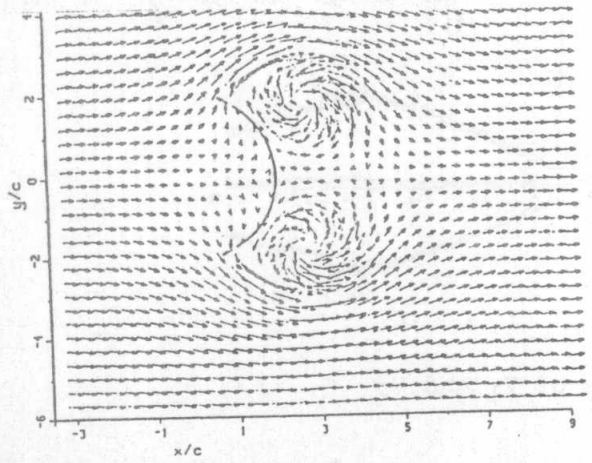

Fig.2. Velocity field at $T^* = 3.5$

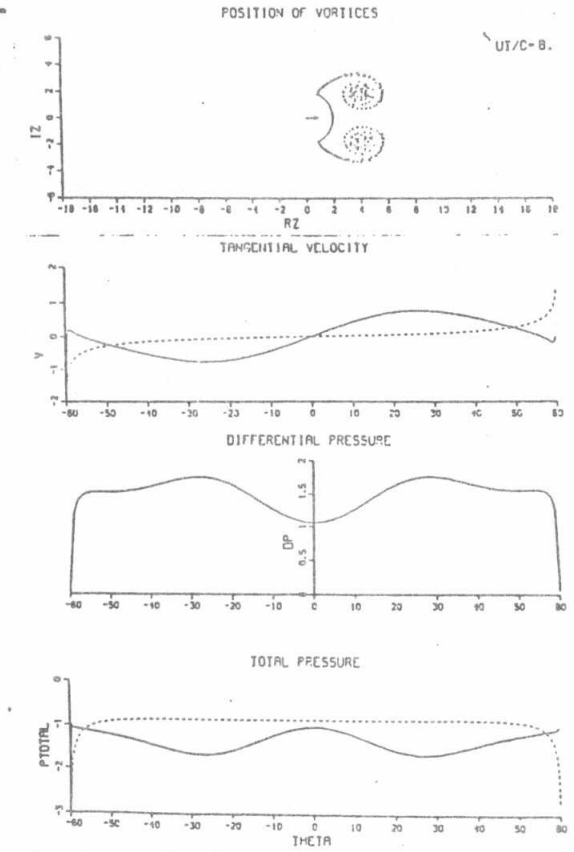

Fig.3. Velocity and Pressure distributions at T^*=8.0

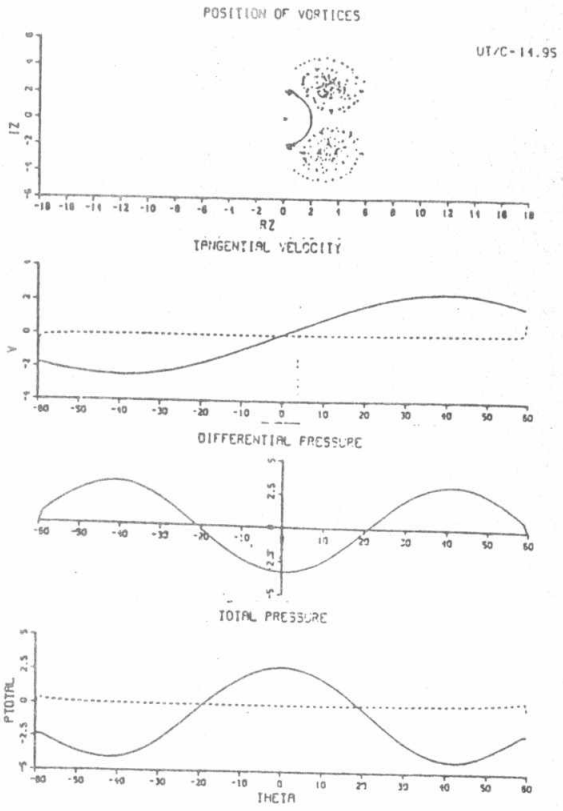

Fig.5. Velocity and Pressure distributions at T^*=14.95

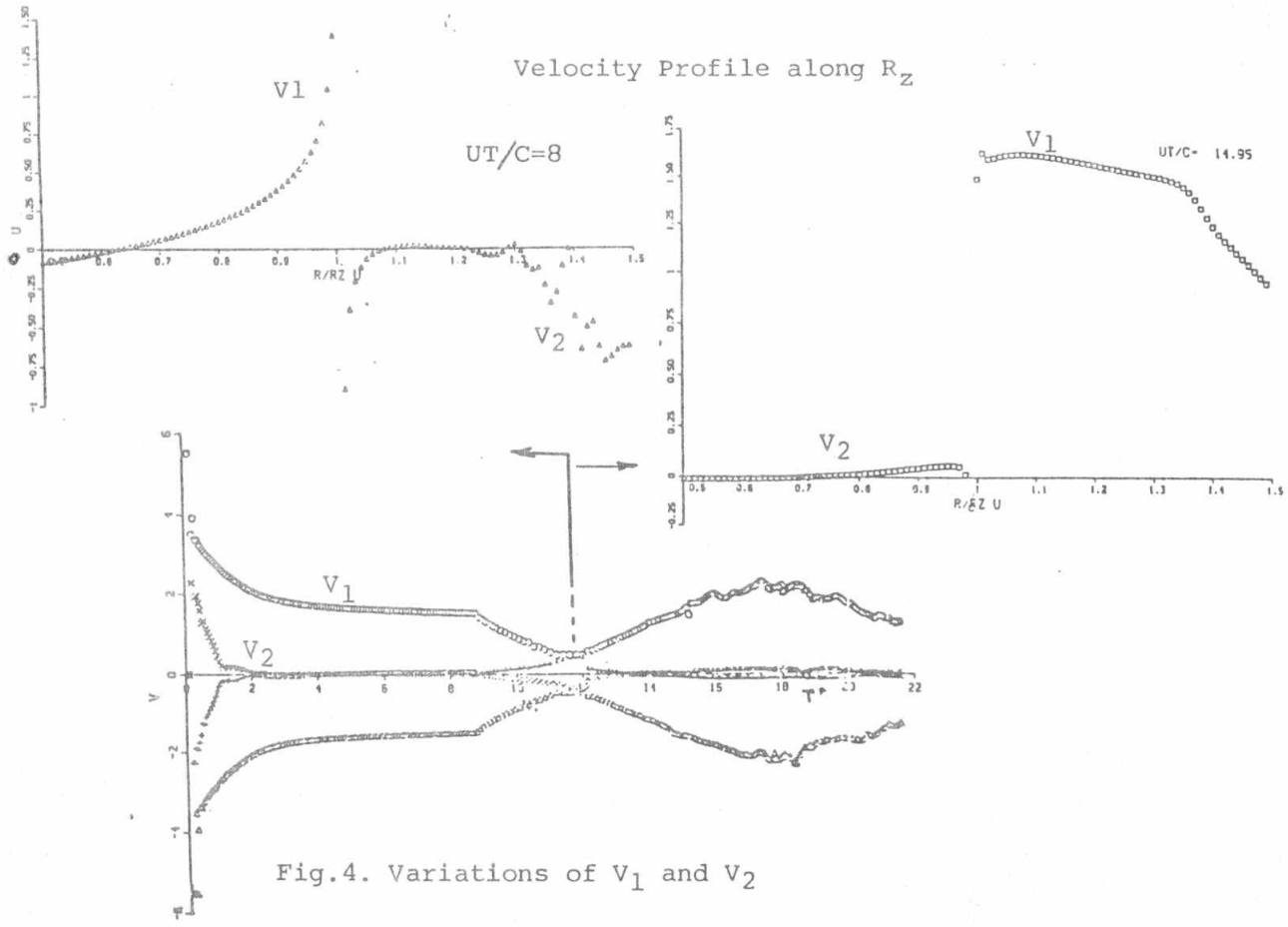

Fig.4. Variations of V_1 and V_2

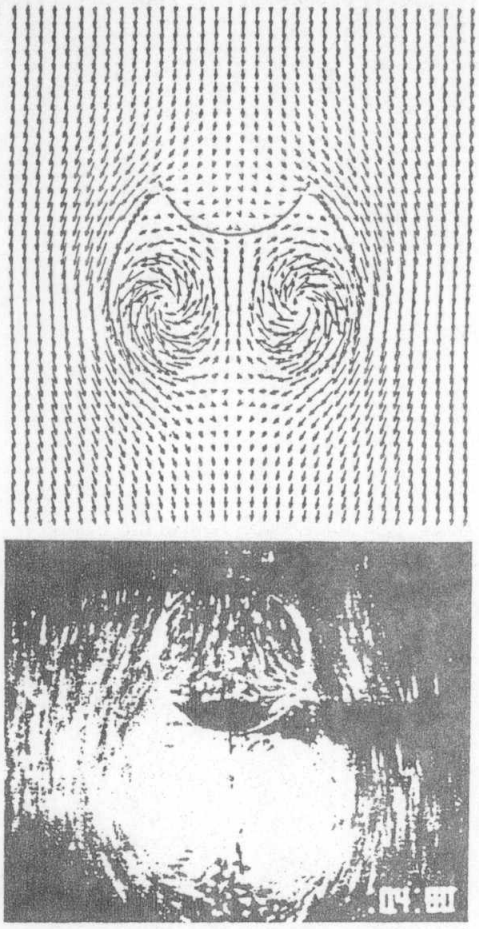

Fig.6. Calculated and photographed flow field at $T^* = 6.05$

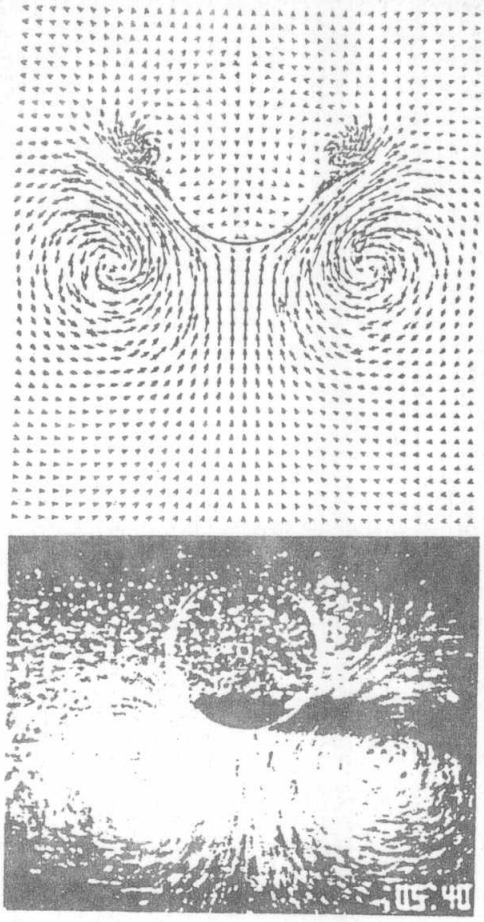

Fig.7. Calculated and photographed flow field at $T^* = 14.$

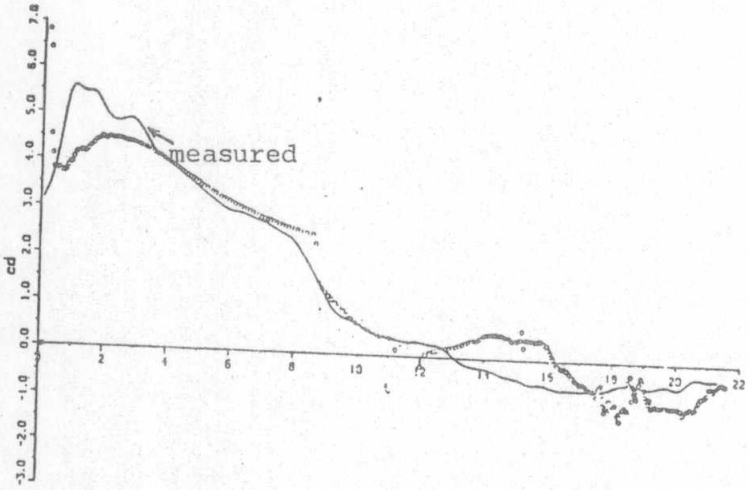

Fig.8. Measured and calculated drag coefficients

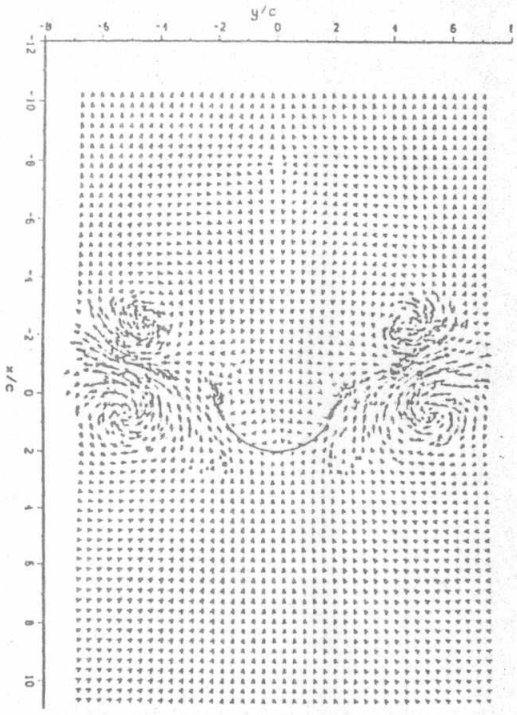

Fig.9. Velocity field at $T^* = 21.5$